International Journal of Heat and Mass Transfer xxx (2016) xxx–xxx

Contents lists available at ScienceDirect

International Journal of Heat and Mass Transfer

journal homepage: www.elsevier.com/locate/ijhmt

Three-dimensional inverse heat conduction modeling of a multi-layered hollow cylindrical tube using input estimation algorithm and thermal resistance network

Jung-Hun Noh [a], Ki-Up Cha [b], Se-Jin Yook [a,*]

[a] School of Mechanical Engineering, Hanyang University, Seoul 133-791, South Korea
[b] 5-1, Agency of Defense Development, Deajeon 305-600, South Korea

ARTICLE INFO

Article history:
Received 6 August 2016
Received in revised form 29 September 2016
Accepted 29 September 2016
Available online xxxx

Keywords:
Inverse heat conduction
Recursive input estimation algorithm
Thermal resistance network
Kalman filter
Multi-layered hollow cylindrical tube

ABSTRACT

High-temperature gas flow can cause melt, crack, erosion, and wear of tubes. In order to reduce these side effects, the inner wall of a hollow cylindrical tube is generally coated with a resistive material, for example, a steel pipe coated with a chrome layer. In addition, it is important to know heat flux applied to the tube wall and temperature distribution in the tube wall for appropriate design of the hollow cylindrical tube. In this study, three-dimensional inverse heat conduction modeling of a multi-layered hollow cylindrical tube was conducted. The thermal resistance network (TRN) scheme was employed to solve the heat conduction in the tube. The temperature distribution in the tube was estimated from a measured temperature on the outer wall of the tube by Kalman filter. At the same time, unknown heat flux on the inner wall of the tube was calculated by the recursive least squares algorithm.

1. Introduction

Recently various analytical methods using numerical analysis have been introduced in various fields of engineering, and studies using these methods are in progress. These achievements resulted from not only the numerical analysis algorithm portraying physical phenomena but also the improvement of process for calculation. In order to predict a physical phenomenon of interest through the numerical analysis, interested region's physical property, boundary condition, and initial condition should be given besides the accurate modeling for the phenomenon. However, different methods of approach should be used instead of the ordinary analysis method if it is difficult to know the boundary conditions of the region being analyzed accurately due to difficulty of the measurement. For example, the direct heat transfer analysis, which is generally used in the field of heat transfer, makes prediction of internal temperature distribution possible because its mathematical modeling as well as boundary and initial conditions for the analyzed region are clear. When a certain boundary condition is unknown, the inverse heat transfer analysis is used to predict the boundary condition and the internal temperature distribution. For the inverse heat transfer analysis, mathematical modeling for the interested region is mandatory, and at the same time, mathematical tools are needed in order to draw physical quantity. Since the inverse heat transfer analysis is mathematically more complicated and requires a lot more numerical costs than the general direct heat transfer analysis, selection of numerical method is important to solve problems more effectively.

Studies on analytical or numerical methods have been done by many researchers for a long time to effectively solve the inverse heat transfer problem. First, as an analytical method, a method for predicting heat flux using heat conduction equation and temperature of two points was introduced. However, it could only analyze steady state condition and linear temperature distribution since it predicted heat flux by integrating heat conduction equation. To improve the weakness, different problem solving method using integral or Laplace transform technique was introduced by many researchers including Stolz [1–5]. However, it also had a limit that it could only analyze one-dimensional unsteady state condition of relatively simple form. As a numerical method, the sequential estimation method has been studied by researchers like Back et al. [6–9], and study of the conjugated gradient method is still in progress by research teams including Alifanov et al. [10–14]. Both the sequential estimation method and the conjugated gradient method are types of recursive calculation method, which is simple and effective, and are most widely used to solve both linear and nonlinear problems. In addition, the recursive

* Corresponding author.
E-mail address: ysjnuri@hanyang.ac.kr (S.-J. Yook).

http://dx.doi.org/10.1016/j.ijheatmasstransfer.2016.09.101
0017-9310/

Nomenclature

A	area, m^2
B	sensitivity matrix
C	capacitance, J/K
$[C]$	capacitance matrix
C_p	specific heat, J/kg·K
E	element number
$\{F\}$	thermal load vector
h	convection heat transfer coefficient, $W/m^2 \cdot K$
H	measurement matrix
I	identity matrix
k	thermal conductivity, W/m·K
K	Kalman gain
K_b	steady-state correction gain
L	length, m
M	sensitivity matrix
$[M]$	conductance matrix
O	error order
P	filter's error covariance matrix
P_b	error covariance matrix
q	heat flux, W/m^2
$\hat{q}$	estimated input vector, W/m^2
Q	process noise covariance
r	circumferential direction
R	measurement noise covariance
Re	thermal resistance, K/W
s	innovation covariance
t	time, s
T	temperature, K
$\{T\}$	temperature vector
T_∞	ambient temperature, K
T_0	initial temperature, K
V	volume, m^3
X	state vector
$\bar{X}$	input estimator
z	length direction
Z	observation vector
$\bar{Z}$	bias innovation

Greek letters

α	thermal diffusivity, m^2/s
γ	forgetting factor
Γ	input matrix
θ	time-stepping scheme parameter
κ	time (discretized), s
Λ	coefficient matrix
ν	measurement noise vector
ρ	density, kg/m^3
ϕ	direction of angle
Φ	state transition matrix
ω	process noise vector

Superscripts

n	time domain

Subscripts

c	chrome
$cond$	conduction
$conv$	convection
f	interface between chrome and steel
H	heat flux
i	inner
l	point number of angle of direction
m	point number of length direction
n	point number of circumferential direction
o	outer
s	steel
$solar$	solar radiation energy
t	tube

input estimation algorithm, *i.e.*, a method for predicting unsteady state condition, provides information of changes in variables on time and draws result that is the closest to actual value of physical quantity by adopting the differences of each variable [15–18].

In this study, analysis of inverse heat transfer through a hollow cylindrical tube is performed with use of the recursive input estimation algorithm. For this study to be performed, numerical heat transfer modeling of the hollow cylindrical tube is needed while, in other existing studies, finite element method was used for system modeling [19–22]. A shortcoming of the finite element method, an existing model, is that numerical costs are very high since it uses so many high-dimensional numerical calculations. In this study, the thermal resistance network method, a type of the finite differential method, is used for heat transfer modeling in order to complement the shortcoming of the finite element method. Some advantages of using the thermal resistance network method are that it has a wide range of applications since it represents the derivative terms, which appear in differential equations, by using Taylor series expansion, and that it has relatively small quantity of numerical calculation. Due to these advantages, the thermal resistance method has been commonly used for the analysis of heat transfer that is used to predict the temperature distribution of steady or unsteady state condition within a motor [23–24].

In this study, development of an analysis model for prediction of heat flux and temperature distribution in the three-dimensional hollow cylindrical tube is performed with use of the inverse heat transfer analysis employing the Kalman filter and the recursive input estimation algorithm. During the process, the thermal resistance method is used for modeling in order to save numerical costs from the existing heat transfer modeling method. The way that the thermal resistance method is applied to the recursive input estimation algorithm is introduced. The inverse heat transfer analysis method that is developed in this study predicts heat flux, which variously changes according to changes in time and position, and proves its validity by comparing its result to the true value. Also, its prediction value of heat flux is compared to the true value when disturbance, such as solar radiation, happens outside the tube in order to evaluate its performance.

2. Model description

In this study, a simple tube as shown in Fig. 1 is used to develop a modeling for the inverse heat transfer analysis of the three-dimensional hollow cylindrical tube. The tube consists of two layers, chrome and steel, for its durability, since fluid with high temperature and pressure is assumed to flow in the tube. The tube's internal diameter, external diameter, and length are denoted as r_i, r_o, and L, respectively, and the interface between the boundaries of chrome and steel layers is denoted as r_f. Due to the flow of fluid with high temperature and pressure in the tube, heat flux, $q(z, \phi, t)$, which is a function of time, the tube's length, and direction of angle, can be calculated. However, it is assumed that the heat flux

Please cite this article in press as: J.-H. Noh et al., Three-dimensional inverse heat conduction modeling of a multi-layered hollow cylindrical tube using input estimation algorithm and thermal resistance network, Int. J. Heat Mass Transfer (2016), http://dx.doi.org/10.1016/j.ijheatmasstransfer.2016.09.101

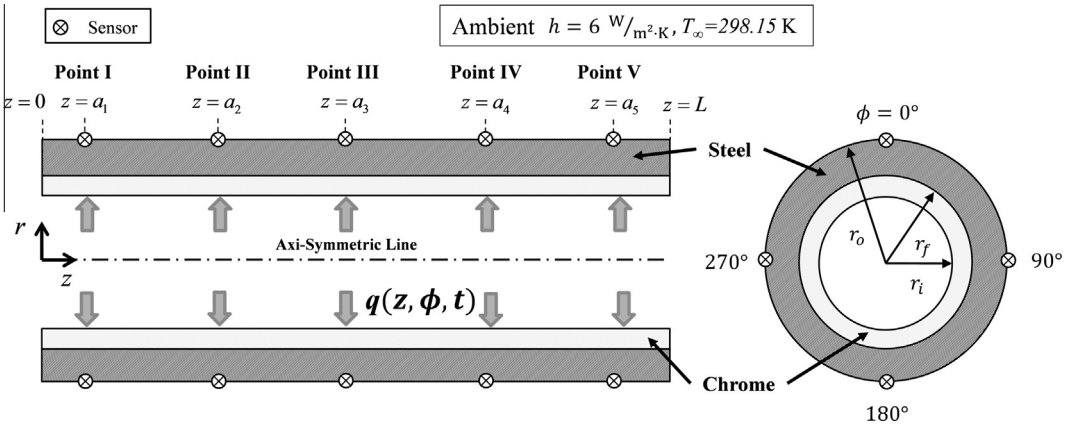

Fig. 1. Schematic diagram for a three-dimensional two-layered hollow cylindrical tube.

on direction of angle is consistent because deviation of heat flux on direction of angle is small. Since the exterior surface of the tube is exposed to air at room temperature, a constant condition of convection current, 6 W/m^2·K, is given as a means of setting up a boundary condition to allow the heat to escape. Sensors marked as ⊗ are attached to the external surface of the tube at regular intervals to measure temperature. A total of twenty sensors are used for the measurement of temperature, including five sensors each in the direction of length and four sensors each in the direction of angle. The values from the sensors are used as input values for the inverse heat transfer analysis and used to predict the internal heat flux of the tube. During the analysis, chrome and steel's physical properties, which include density, thermal conductivity, and specific heat, are considered constant, and the thermal resistance between chrome and steel is neglected. Under these conditions and assumptions, governing equations concerning the heat conduction of the tube are as follows:

Governing equation of three-dimensional transient heat conduction [25]:

$$\frac{\partial^2 T(r,z,\phi,t)}{\partial r^2}+\frac{1}{r}\frac{\partial T(r,z,\phi,t)}{\partial r}+\frac{1}{r^2}\frac{\partial^2 T(r,z,\phi,t)}{\partial \phi^2}+\frac{\partial^2 T(r,z,\phi,t)}{\partial z^2} = \left(\frac{1}{\alpha_c}\right)\frac{\partial T(r,z,\phi,t)}{\partial t}, \quad \text{for } r_i \leqslant r \leqslant r_f \tag{1}$$

$$\frac{\partial^2 T(r,z,\phi,t)}{\partial r^2}+\frac{1}{r}\frac{\partial T(r,z,\phi,t)}{\partial r}+\frac{1}{r^2}\frac{\partial^2 T(r,z,\phi,t)}{\partial \phi^2}+\frac{\partial^2 T(r,z,\phi,t)}{\partial z^2} = \left(\frac{1}{\alpha_s}\right)\frac{\partial T(r,z,\phi,t)}{\partial t}, \quad \text{for } r_f \leqslant r \leqslant r_o \tag{2}$$

Initial conditions:

$$T(r,z,\phi,t) = T_0, \text{ at } \quad t = 0, \text{ for } r_i \leqslant r \leqslant r_o, 0° \leqslant \phi < 360° \text{ and } 0 \leqslant z \leqslant L_t \tag{3}$$

Boundary conditions:

$$-k_c\frac{\partial T(r,z,\phi,t)}{\partial r} = q(z,\phi,t), \text{ for } r = r_i,\ 0° \leqslant \phi < 360° \text{ and } 0 \leqslant z \leqslant L_t \tag{4}$$

$$-k_s\frac{\partial T(r,z,\phi,t)}{\partial r} = h[T(r,z,\phi,t) - T_\infty], \text{ for } r = r_o,\ 0° \leqslant \phi < 360° \text{ and } 0 \leqslant z \leqslant L_t \tag{5}$$

$$-k_c\frac{\partial T(r,z,\phi,t)}{\partial r} = h[T(r,z,\phi,t) - T_\infty], \quad \text{for } r_i \leqslant r \leqslant r_f,\ 0° \leqslant \phi < 360°, z = 0 \text{ and } z = L_t \tag{6}$$

$$-k_s\frac{\partial T(r,z,\phi,t)}{\partial r} = h[T(r,z,\phi,t) - T_\infty], \quad \text{for } r_f \leqslant r \leqslant r_o,\ 0° \leqslant \phi < 360°, z = 0 \text{ and } z = L_t \tag{7}$$

$$k_c\left(\frac{\partial T(r,z,\phi,t)}{\partial r}\right)_c = k_s\left(\frac{\partial T(r,z,\phi,t)}{\partial r}\right)_s \text{ for } r = r_f,\ 0° \leqslant \phi < 360° \text{ and } 0 \leqslant z \leqslant L_t \tag{8}$$

In this study, the thermal resistance network is used for the heat transfer modeling. The thermal resistance network is a theory that applies the concept of electric resistance to the heat transfer by using the similarity. Composition of the thermal resistance network using the thermal resistance method is shown in Fig. 2. The resistance equations of conduction (Re_{cond}) and convection (Re_{conv}) between each point on directions of length and angle are as follows [25]:

$$\mathrm{Re}_{cond,r} = \frac{\ln\left(\frac{r_{n+1}}{r_n}\right)}{2\pi Lk} \tag{9}$$

$$\mathrm{Re}_{cond,z} = \frac{L}{kA} \tag{10}$$

$$\mathrm{Re}_{cond,\phi} = \frac{L}{kA} \tag{11}$$

$$\mathrm{Re}_{conv,r} = \frac{1}{2\pi r_o Lh} \tag{12}$$

$$\mathrm{Re}_{conv,z} = \frac{1}{hA} \tag{13}$$

$$\mathrm{Re}_{conv,\phi} = \frac{1}{hA} \tag{14}$$

This analysis model shows the analysis of unsteady state condition that examines changes on time. Accordingly, modeling for the unsteady state analysis is needed, and it can be performed through the addition of terms of thermal capacity. The equation for this is expressed as follows:

$$C = \rho V C_p \tag{15}$$

Under the governing equations and the boundary conditions mentioned above, the relationship between points can be expressed by the thermal resistance equations that are shown below. First, the equations for the tube's internal surface that is directly affected by heat flux are as follows:

$$Aq(z,\phi,t) + \frac{T_{l,m,n} - T_\infty}{\mathrm{Re}_{l,m-1,n,conv}} + \frac{T_{l,m,n} - T_{l,m,n-1}}{\mathrm{Re}_{l,m,n-1,cond}}$$

Please cite this article in press as: J.-H. Noh et al., Three-dimensional inverse heat conduction modeling of a multi-layered hollow cylindrical tube using input estimation algorithm and thermal resistance network, Int. J. Heat Mass Transfer (2016), http://dx.doi.org/10.1016/j.ijheatmasstransfer.2016.09.101

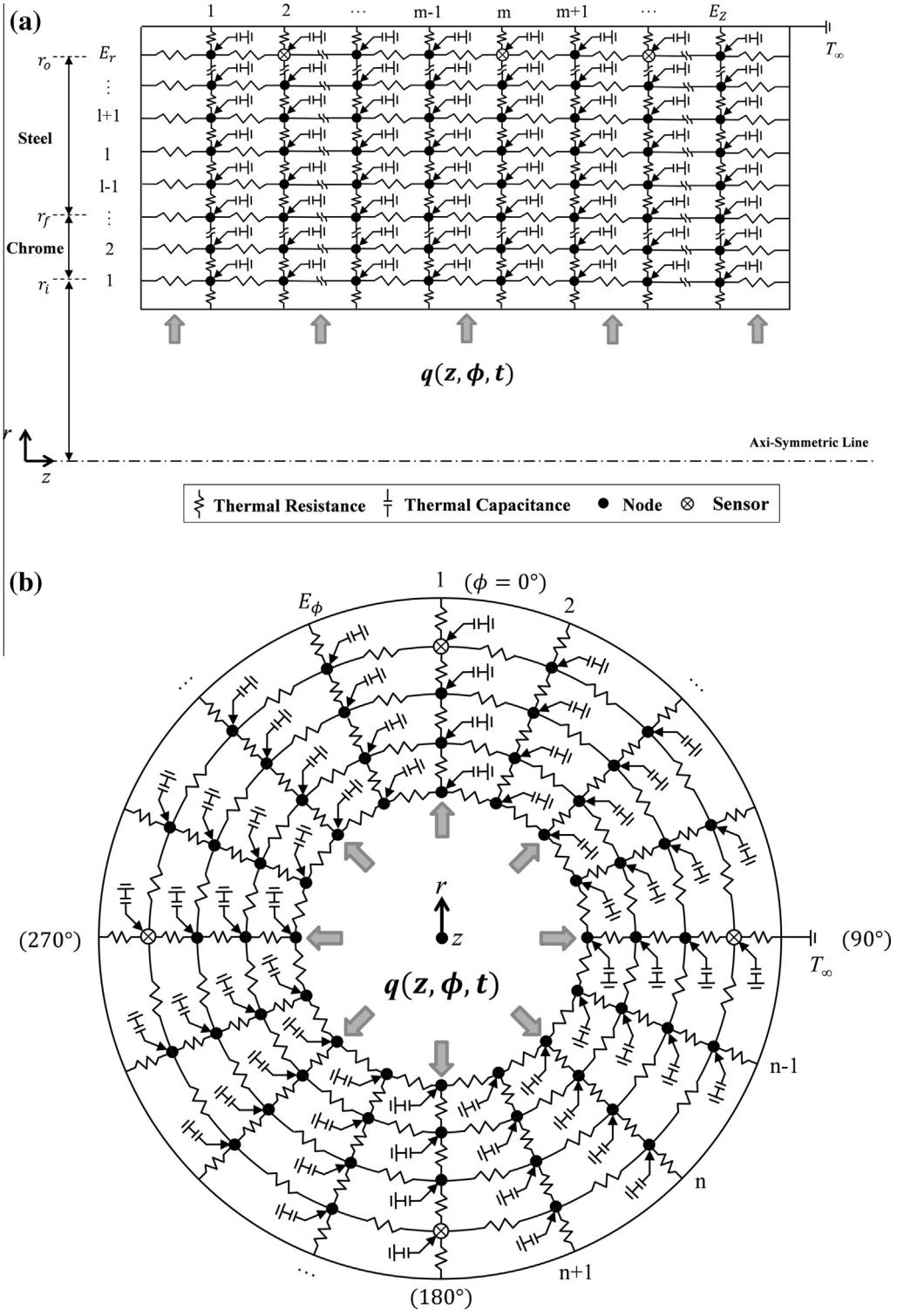

Fig. 2. Thermal resistance network for the three-dimensional two-layered hollow cylindrical tube; (a) side view, (b) front view.

$$= C\frac{\partial\{T\}}{\partial t} + \frac{T_{l+1,m,n} - T_{l,m,n}}{\mathrm{Re}_{l+1,m,n,cond}} + \frac{T_{l,m+1,n} - T_{l,m,n}}{\mathrm{Re}_{l,m+1,n,cond}} + \frac{T_{l,m,n+1} - T_{l,m,n}}{\mathrm{Re}_{l,m,n+1,cond}},$$

for $z = 0$ (16)

$$Aq(z,\phi,t) + \frac{T_{l,m,n} - T_{l,m-1,n}}{\mathrm{Re}_{l,m-1,n,cond}} + \frac{T_{l,m,n} - T_{l,m,n-1}}{\mathrm{Re}_{l,m,n-1,cond}}$$

$$= C\frac{\partial\{T\}}{\partial t} + \frac{T_{l+1,m,n} - T_{l,m,n}}{\mathrm{Re}_{l+1,m,n,cond}} + \frac{T_{l,m+1,n} - T_{l,m,n}}{\mathrm{Re}_{l,m+1,n,cond}} + \frac{T_{l,m,n+1} - T_{l,m,n}}{\mathrm{Re}_{l,m,n+1,cond}},$$

for $0 < z < L_t$ (17)

$$Aq(z,\phi,t) + \frac{T_{l,m,n} - T_{l,m-1,n}}{\mathrm{Re}_{l,m-1,n,cond}} + \frac{T_{l,m,n} - T_\infty}{\mathrm{Re}_{l,m,n-1,conv}}$$

Please cite this article in press as: J.-H. Noh et al., Three-dimensional inverse heat conduction modeling of a multi-layered hollow cylindrical tube using input estimation algorithm and thermal resistance network, Int. J. Heat Mass Transfer (2016), http://dx.doi.org/10.1016/j.ijheatmasstransfer.2016.09.101

$$= C\frac{\partial\{T\}}{\partial t} + \frac{T_{l+1,m,n} - T_{l,m,n}}{\mathrm{Re}_{l+1,m,n,cond}} + \frac{T_{l,m+1,n} - T_{l,m,n}}{\mathrm{Re}_{l,m+1,n,cond}} + \frac{T_{l,m,n+1} - T_{l,m,n}}{\mathrm{Re}_{l,m,n+1,cond}},$$
for $z = L_t$ (18)

The equations for the tube's internal solid area that is not affected directly by the internal and external environment of the tube are as follows:

$$\frac{T_{l,m,n} - T_{l-1,m,n}}{\mathrm{Re}_{l-1,m,n,cond}} + \frac{T_{l,m,n} - T_{\infty}}{\mathrm{Re}_{l,m-1,n,conv}} + \frac{T_{l,m,n} - T_{l,m,n-1}}{\mathrm{Re}_{l,m,n-1,cond}}$$

$$= C\frac{\partial\{T\}}{\partial t} + \frac{T_{l+1,m,n} - T_{l,m,n}}{\mathrm{Re}_{l+1,m,n,cond}} + \frac{T_{l,m+1,n} - T_{l,m,n}}{\mathrm{Re}_{l,m+1,n,cond}} + \frac{T_{l,m,n+1} - T_{l,m,n}}{\mathrm{Re}_{l,m,n+1,cond}},$$
for $z = 0$ (19)

$$\frac{T_{l,m,n} - T_{l-1,m,n}}{\mathrm{Re}_{l-1,m,n,cond}} + \frac{T_{l,m,n} - T_{l,m-1,n}}{\mathrm{Re}_{l,m-1,n,cond}} + \frac{T_{l,m,n} - T_{l,m,n-1}}{\mathrm{Re}_{l,m,n-1,cond}}$$

$$= C\frac{\partial\{T\}}{\partial t} + \frac{T_{l+1,m,n} - T_{l,m,n}}{\mathrm{Re}_{l+1,m,n,cond}} + \frac{T_{l,m+1,n} - T_{l,m,n}}{\mathrm{Re}_{l,m+1,n,cond}} + \frac{T_{l,m,n+1} - T_{l,m,n}}{\mathrm{Re}_{l,m,n+1,cond}},$$
for $0 < z < L_t$ (20)

$$\frac{T_{l,m,n} - T_{l-1,m,n}}{\mathrm{Re}_{l-1,m,n,cond}} + \frac{T_{l,m,n} - T_{l,m-1,n}}{\mathrm{Re}_{l,m-1,n,cond}} + \frac{T_{l,m,n} - T_{\infty}}{\mathrm{Re}_{l,m,n-1,conv}}$$

$$= C\frac{\partial\{T\}}{\partial t} + \frac{T_{l+1,m,n} - T_{l,m,n}}{\mathrm{Re}_{l+1,m,n,cond}} + \frac{T_{l,m+1,n} - T_{l,m,n}}{\mathrm{Re}_{l,m+1,n,cond}} + \frac{T_{l,m,n+1} - T_{l,m,n}}{\mathrm{Re}_{l,m,n+1,cond}},$$
for $z = L_t$ (21)

Lastly, the equations for the tube's external surface that is affected by the convection and solar radiation are as follows:

$$\frac{T_{l,m,n} - T_{l-1,m,n}}{\mathrm{Re}_{l-1,m,n,cond}} + \frac{T_{l,m,n} - T_{\infty}}{\mathrm{Re}_{l,m-1,n,conv}} + \frac{T_{l,m,n} - T_{l,m,n-1}}{\mathrm{Re}_{l,m,n-1,cond}}$$

$$= C\frac{\partial\{T\}}{\partial t} + \frac{T_{\infty} - T_{l,m,n}}{\mathrm{Re}_{l+1,m,n,conv}} + \frac{T_{l,m+1,n} - T_{l,m,n}}{\mathrm{Re}_{l,m+1,n,cond}} + \frac{T_{l,m,n+1} - T_{l,m,n}}{\mathrm{Re}_{l,m,n+1,cond}} + Aq_{solar},$$
for $z = 0$ (22)

$$\frac{T_{l,m,n} - T_{l-1,m,n}}{\mathrm{Re}_{l-1,m,n,cond}} + \frac{T_{l,m,n} - T_{l,m-1,n}}{\mathrm{Re}_{l,m-1,n,cond}} + \frac{T_{l,m,n} - T_{l,m,n-1}}{\mathrm{Re}_{l,m,n-1,cond}}$$

$$= C\frac{\partial\{T\}}{\partial t} + \frac{T_{\infty} - T_{l,m,n}}{\mathrm{Re}_{l+1,m,n,conv}} + \frac{T_{l,m+1,n} - T_{l,m,n}}{\mathrm{Re}_{l,m+1,n,cond}} + \frac{T_{l,m,n+1} - T_{l,m,n}}{\mathrm{Re}_{l,m,n+1,cond}} + Aq_{solar},$$
for $0 < z < L_t$ (23)

$$\frac{T_{l,m,n} - T_{l-1,m,n}}{\mathrm{Re}_{l-1,m,n,cond}} + \frac{T_{l,m,n} - T_{l,m-1,n}}{\mathrm{Re}_{l,m-1,n,cond}} + \frac{T_{l,m,n} - T_{\infty}}{\mathrm{Re}_{l,m,n-1,conv}}$$

$$= C\frac{\partial\{T\}}{\partial t} + \frac{T_{\infty} - T_{l,m,n}}{\mathrm{Re}_{l+1,m,n,conv}} + \frac{T_{l,m+1,n} - T_{l,m,n}}{\mathrm{Re}_{l,m+1,n,cond}} + \frac{T_{l,m,n+1} - T_{l,m,n}}{\mathrm{Re}_{l,m,n+1,cond}} + Aq_{solar},$$
for $z = L_t$ (24)

The modeling for the system between points using the thermal resistance method can be expressed as a form a matrix which is as follows:

$$[C]\frac{\partial\{T\}}{\partial t} + [M]\{T\} + \{F_H\} + \{F_{conv}\} = 0 \quad (25)$$

Here $\{T\}$ refers to the temperature vector that expresses temperature of each point, and $[C]$ refers to the capacitance matrix for expression of the abnormal condition. $[M]$ refers to the conductance matrix for expression of heat conduction of chrome and steel, and $[F_H]$ refers to the thermal load vector of heat flux that expresses heat flux of the tube's surface. Lastly, $\{F_{conv}\}$ refers to the thermal load vector of convection expressing the tube's external convection.

In order to numerically solve the term of the unsteady state condition as expressed in Eq. (25), Taylor series is used to express the difference on time [26]. The expression is as follows:

$$\frac{\partial T^n}{\partial t} \approx \frac{T^{n+1} - T^n}{\Delta t} + O(\Delta T) \quad (26)$$

Here t refers to time, and Δt refers to sampling interval. The equation for time difference on temperature can be obtained after arranging Eq. (26) by adopting a time-stepping parameter, θ.

$$T^{n+\theta} = \theta T^{n+1} + (1-\theta)T^n \quad (27)$$

The method for the difference on time can be altered according to changes in the value of θ. When $\theta = 0.0$, $\theta = 0.5$, and $\theta = 1.0$, it is set up as fully explicit scheme (forward difference method), semi-implicit scheme (Crank-Nicolson method), and fully implicit scheme (backward difference method), respectively.

Rearrangement of Eq. (25) by combining it with Eqs. (26) and (27) that have been induced initially is as follows:

$$[C]\left\{\frac{T^{n+1} + T^n}{\Delta t}\right\} + [M]\left\{\theta T^{n+1} + (1-\theta)T^n\right\} + \left\{\theta F_H^{n+1} + (1-\theta)F_H^n\right\} + \{F_{conv}^n\} = 0 \quad (28)$$

Here $\{F_{conv}^n\} = \{F_{conv}^{n+1}\}$ is achieved since the condition of external convection of the tube is assumed to be always constant. In this study, among methods for difference on time, the fully implicit scheme is used, *i.e.*, $\theta = 1.0$. Therefore, conversion of Eq. (28) to a state equation on time can be expressed as follows:

$$X(\kappa) = \Phi X(\kappa-1) + \Gamma_1[q(\kappa) + \omega(\kappa)] + \Gamma_2[q(\kappa-1) + \omega(\kappa-1)] + \Lambda h \quad (29)$$

Here X refers to state vector, Φ refers to state transition matrix, and κ refers to time. In addition, Γ_1 and Γ_2 both refer to input matrix, and q (heat flux) refers to deterministic input sequence. Also, ω refers to process noise vector, and Λ refers to coefficient matrix. Each matrix of X, Φ, Γ_1, Γ_2, and Λ is as follows:

$$X(\kappa-1) = \{T_1, T_2, T_3, \cdots T_{N-2}, T_{N-1}, T_N\} \quad (30)$$

$$\Phi = ([C] + \theta\Delta t[M])^{-1}([C] - (1-\theta)\Delta t[M]) \quad (31)$$

$$\Gamma_1 = -\theta\Delta t([C] + \theta\Delta t[M])^{-1}\{F_H^{n+1}\} \quad (32)$$

$$\Gamma_2 = -(1-\theta)\Delta t([C] + \theta\Delta t[M])^{-1}\{F_H^n\} \quad (33)$$

$$\Lambda = -\Delta t([C] + \theta\Delta t[M])^{-1}\{F_{conv}\} \quad (34)$$

In order to predict heat flux by using measured temperature information, the inverse heat transfer analysis method of the input estimation approach needs to be used. This method can be divided into two parts: Kalman filter and recursive least-squares algorithm. A concrete explanation of inducing process algorithm is shown in the references [19,22,27]. First, calculation process of the Kalman filter is as follows:

$$\bar{X}(\kappa/\kappa-1) = \Phi\bar{X}(\kappa-1/\kappa-1) + \Lambda h \quad (35)$$

$$P(\kappa/\kappa-1) = \Phi P(\kappa-1/\kappa-1)\Phi^T + \Gamma_1 Q\Gamma_1^T + \Gamma_2 Q\Gamma_2^T \quad (36)$$

$$s(\kappa) = HP(\kappa/\kappa-1)H^T + R \quad (37)$$

Please cite this article in press as: J.-H. Noh et al., Three-dimensional inverse heat conduction modeling of a multi-layered hollow cylindrical tube using input estimation algorithm and thermal resistance network, Int. J. Heat Mass Transfer (2016), http://dx.doi.org/10.1016/j.ijheatmasstransfer.2016.09.101

$$K(\kappa) = P(\kappa/\kappa-1)H^T s^{-1}(\kappa) \tag{38}$$

$$P(\kappa/\kappa) = [I - K(\kappa)H]P(\kappa/\kappa-1) \tag{39}$$

$$\bar{Z}(\kappa) = Z(\kappa) - H\bar{X}(\kappa/\kappa-1) \tag{40}$$

$$\bar{X}(\kappa/\kappa) = \bar{X}(\kappa/\kappa-1) + K(\kappa)\bar{Z}(\kappa) \tag{41}$$

Here $\bar{X}$ refers to the input estimator, and P refers to the filter's error covariance matrix. Q refers to the process noise covariance, s refers to the innovation covariance, and H refers to the measurement matrix. In addition, R refers to the measurement noise covariance, Z refers to the observation matrix, and $\bar{Z}$ refers to the bias innovation.

Calculation process of the recursive least-squares algorithm is as follows:

$$B(\kappa) = H[\Phi M(\kappa-1) + I]\Gamma_1 + H[\Phi M(\kappa-1) + I]\Gamma_2 \tag{42}$$

$$M(\kappa) = [I - K(\kappa)H][\Phi M(\kappa-1) + I] \tag{43}$$

$$K_b(\kappa) = \gamma^{-1}P_b(\kappa-1)B^T(\kappa)[B(\kappa)\gamma^{-1}P_b(\kappa-1)B^T(\kappa) + s(\kappa)]^{-1} \tag{44}$$

$$P_b(\kappa) = [I - K_b(\kappa)B(\kappa)]\gamma^{-1}P_b(\kappa-1) \tag{45}$$

$$\hat{q}(\kappa) = \hat{q}(\kappa-1) + K_b(\kappa)[\bar{Z}(\kappa) - B(\kappa)\hat{q}(\kappa-1)] \tag{46}$$

Here B and M both refer to the sensitivity matrices, and I refers to the identity matrix. K_b refers to the correction gain, and γ refers to the forgetting factor. In addition, P_b refers to the error covariance of estimated input vector, and $\hat{q}(\kappa)$ refers to the estimated input vector.

Fig. 3 is a diagram that shows the process of the inverse heat transfer analysis performed in this study. Numerical methods are used to verify the validity of the analysis model developed in this study. Errors can be confirmed through comparison between the input value, $q(\kappa)$, of heat flux on time change and predicted result value, $\hat{q}(\kappa)$. The direct heat transfer analysis is performed with use of the ANSYS FLUENT *Release 16.1*, a commercial program, in order to obtain the measured value of temperature, $Z(\kappa)$, of the tube's external surface. The value of temperature obtained through the process is used as the input value for the inverse heat transfer analysis, and heat flux of the tube's internal surface is predicted through the input estimation algorithm. For the process, the thermal resistance network method is used for the inverse heat transfer modeling. The input estimation algorithm is composed of the Kalman filter and the recursive least square algorithm. The equation to find the observation matrix is as follows:

$$Z(\kappa) = HX(\kappa) + v(\kappa) \tag{47}$$

Here Z refers to observation vector, H refers to measurement matrix, and v refers to measurement noise vector.

3. Results and discussion

Information of shape and location of temperature sensors for the analysis of the three-dimensional hollow cylindrical tube model are provided in Table 1. Information of shape is provided based on the fact that the hollow cylindrical tube is composed of two different materials. In addition, locations for measurement of temperature are provided since measurement of temperature on the tube's surface is performed for the inverse heat transfer analysis. Table 2 shows properties of matter of materials that constitute the hollow cylindrical tube and the tube's external boundary condition. For each property of matter, materials that are used in actual production of hollow cylindrical tube are measured. On the other hand, the external boundary conditions are selected

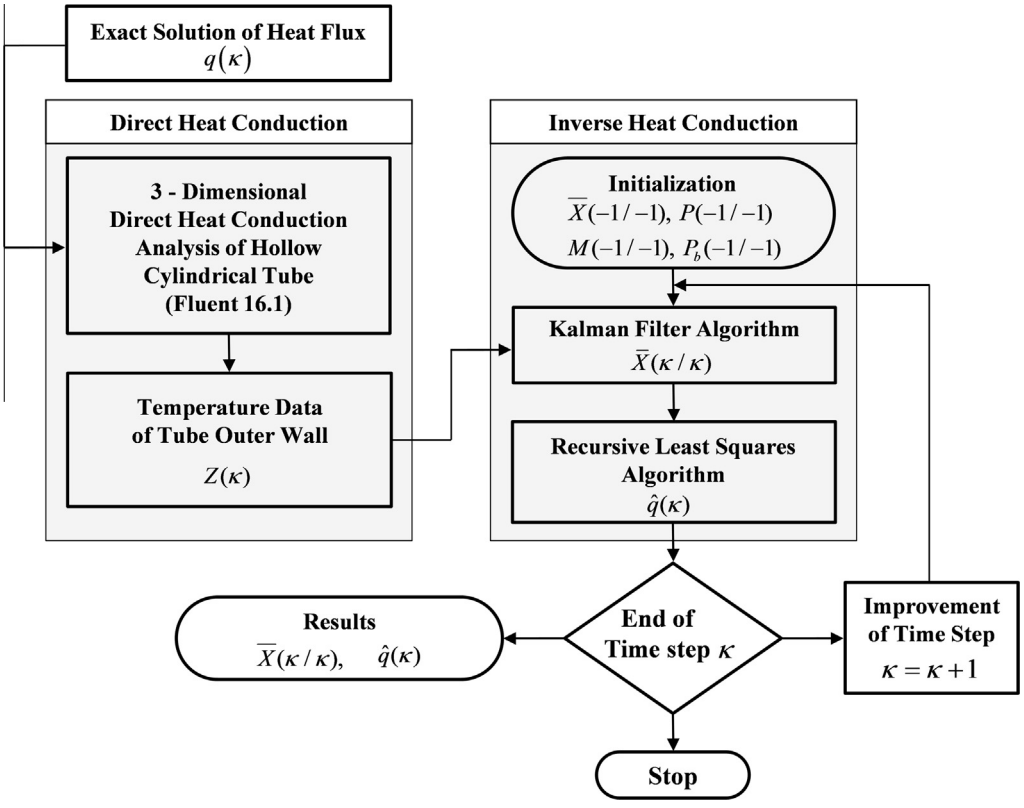

Fig. 3. Flow chart of the numerical analysis.

Please cite this article in press as: J.-H. Noh et al., Three-dimensional inverse heat conduction modeling of a multi-layered hollow cylindrical tube using input estimation algorithm and thermal resistance network, Int. J. Heat Mass Transfer (2016), http://dx.doi.org/10.1016/j.ijheatmasstransfer.2016.09.101

Table 1
Geometrical parameter and sensing location of two-layered hollow cylindrical tube.

Description		Symbol	Value	Unit
Dimensions	Inner radius	r_i	0.020	m
	Radial position of the interface	r_f	0.021	m
	Outer radius	r_o	0.040	m
	Length	L	2.000	m
Temperature measurement points	Point I	a_1	0.200	m
	Point II	a_2	0.600	m
	Point III	a_3	1.000	m
	Point IV	a_4	1.400	m
	Point V	a_5	1.800	m

Table 2
Material properties and boundary conditions of two-layered hollow cylindrical tube.

Description		Symbol	Value	Unit
Material properties	Density of steel	ρ_s	8052	kg/m^3
	Density of chrome	ρ_c	7160	kg/m^3
	Thermal conductivity of steel	k_s	40.4	W/m-K
	Thermal conductivity of chrome	k_c	93.7	W/m-K
	Specific heat of steel	$C_{p,s}$	426.0	J/kg-K
	Specific heat of chrome	$C_{p,c}$	449.0	J/kg-K
Boundary conditions	Convection coefficient of outer wall	h_o	6.0	W/m^2-K
	Atmosphere temperature	T_∞	298.15	K

based on the existing reference related to inverse heat transfer [27].

Since the effect of process noise covariance and measurement noise covariance on input estimation algorithm is big, selecting appropriate values for each analysis model is necessary. However, since the effect on value and the range of appropriate value are provided in the preceding study [27], results can be drawn from the assumption that process noise covariance is $Q = 10$, measurement noise covariance is $\sigma = 10^{-3}$, and forgetting factor is $\gamma = 0.925$. In addition, it is assumed that sampling interval for the progress of numerical analysis is $\Delta t = 0.01s$, the number of element on the circumferential direction is $E_r = 5$, the number of elements on the direction of length is $E_z = 50$, and the number of elements on the direction of angle is $E_\phi = 8$. Temperature of the hollow cylindrical tube and the external environment in the initial state before the application of heat flux is $T_0 = 298.15K$, and temperature of external air is consistent with the initial temperature.

For the analysis, heat flux of simple square wave that changes only on time and is constant on the direction of length is expressed in Eq. (48) below:

$$q(z,\phi,t) = \begin{cases} 0 & \text{for } 0 \leqslant t < 5, 15 \leqslant t \leqslant 30 \\ & \quad 0 \leqslant z \leqslant 2.0, 0^\circ \leqslant \phi < 360^\circ \\ 700,0000 & \text{for } 5 \leqslant t < 15 \\ & \quad 0 \leqslant z \leqslant 2.0, 0^\circ \leqslant \phi < 360^\circ \end{cases} \tag{48}$$

Fig. 4 shows the comparison between the actual values that are provided when heat flux is supplied to inner wall of the hollow cylindrical tube and the predicted values through the inverse heat transfer analysis. While Fig. 4a is a graph that shows the comparison of heat flux of sensor fixed on 0 degree among varying measurement locations on the direction of length, Fig. 4b shows the comparison of heat flux of varying angle directions of the sensor located at Point III in the direction of length. As shown in Fig. 4, it is confirmed that the predicted value of heat flux in the same direction of length and angle corresponds to the tendency of actually supplied value. However, when it is compared to the findings in the existing literature [28,29], a considerable amount of delay is confirmed until approaching the true value. It is confirmed that the delay is due to the effects that occur as the thickness of the analysis model shape increases, not the numerical difference on the expansion of model dimension. In other words, time for heat transfer increases as the thickness of solid with the same property of matter increases, and this effect is expressed as delay of the inverse heat transfer. If the difference of stabilization of the predicted value compared to actually supplied heat flux is set to ±1.00%, the delay time for the stabilization is 1.01 s.

The pattern of heat flux of square wave that changes according to time and the length direction of the hollow cylindrical tube is expressed in Eq. (49) below.

$$q(z,\phi,t) = \begin{cases} 0 & \text{for } 0 \leqslant t < 2 \\ & \quad 0 \leqslant z \leqslant 2.0, 0^\circ \leqslant \phi < 360^\circ \\ 1.135 \cdot 10^7 \cdot c \cdot e^{-(0.8333+z)} \cdot \frac{b}{a}\left(\frac{3}{a}\right)^{b-1} \cdot e^{-\left(\frac{3}{a}\right)^b} & \text{for } 2 \leqslant t \leqslant 30 \\ & \quad 0 \leqslant z \leqslant 2.0, 0^\circ \leqslant \phi < 360^\circ \end{cases} \tag{49}$$

Here fitting constants are $a = 4.8$ and $b = 1.8$. The value of both floor function c and fitting constant d are shown in Eq. (50) and Eq. (51) below.

$$c = \left\lfloor -\frac{2d}{t+d} + 2 \right\rfloor - \left\lfloor -\frac{2(12+d)}{t+12+d} + 2 \right\rfloor \tag{50}$$

$$d = 1 + \frac{z}{0.2} \tag{51}$$

Fig. 5 shows the predicted result through the inverse heat transfer analysis when heat flux of square wave that changes in the direction of both time and length is supplied. As shown in Fig. 5a, it is confirmed that it is possible to predict the tendency of the phenomenon even though changes of heat flux in the direction of length occur. However, it is also confirmed that a delay exists until the actually provided heat flux reaches the true value just like the earlier findings. If standard of error for stabilization is set to ±1.00%, the maximum time for stabilization is 1.02 s. Fig. 5b shows

Please cite this article in press as: J.-H. Noh et al., Three-dimensional inverse heat conduction modeling of a multi-layered hollow cylindrical tube using input estimation algorithm and thermal resistance network, Int. J. Heat Mass Transfer (2016), http://dx.doi.org/10.1016/j.ijheatmasstransfer.2016.09.101

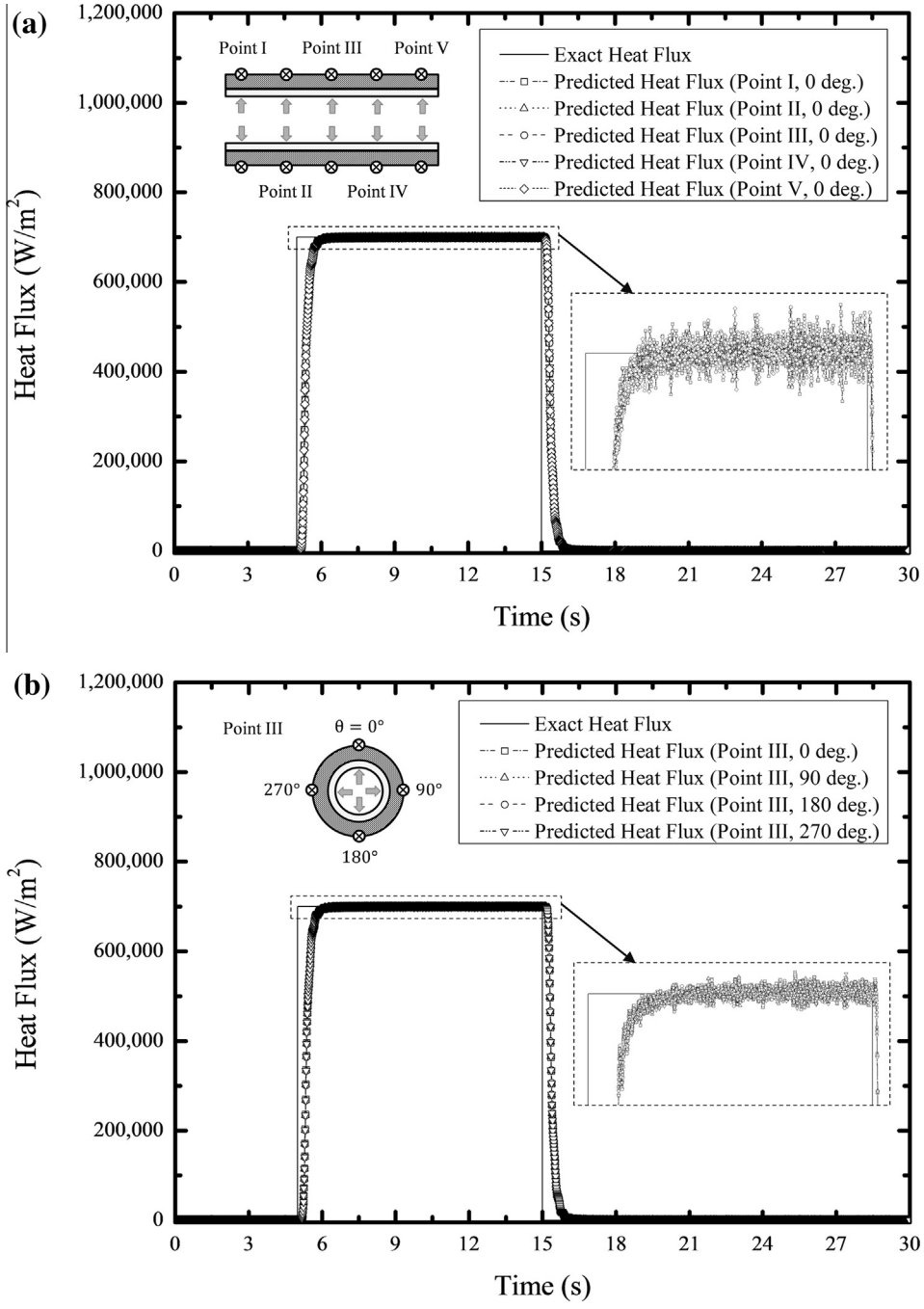

Fig. 4. Comparison between the exact heat flux profile of simple square wave that changes according to time and the heat flux predicted by the numerical model; (a) length direction, (b) angle direction.

the comparison of predicted values of heat flux according to varying angle directions of the sensor located at Point III in the direction of length. The same level of predicted value is confirmed since all the heat flux of angle direction is constant in the same direction of length. Moreover, it is confirmed that time for the stabilization is 0.92 s.

While the inverse heat transfer analysis on square wave form and its results are discussed in the preceding cases, predicted results on sine wave form are discussed in this case. First of all, the form of heat flux of sinusoidal-like wave form that changes according to time and the length direction of hollow cylindrical tube is expressed in Eq. (52) below.

$$q(z,\phi,t)=\begin{cases}0 & \text{for } 0\leqslant t<\mathrm{d}\\ & 0\leqslant z\leqslant 2.0, 0^\circ\leqslant\phi<360^\circ\\ 1.135\cdot 10^7\cdot e^{-(0.8333+z)} & \\ \cdot\frac{b}{a}\left(\frac{t-d}{a}\right)^{b-1}\cdot e^{-\left(\frac{t-d}{a}\right)^b} & \text{for } \mathrm{d}\leqslant t\leqslant 30\\ & 0\leqslant z\leqslant 2.0, 0^\circ\leqslant\phi<360^\circ\end{cases} \tag{52}$$

Here the fitting constants are $a = 4.8$ and $b = 1.8$. The fitting constant d is calculated by Eq. (51). As shown in Fig. 6a, it is confirmed that the tendency of the predicted result of sinusoidal-like

Please cite this article in press as: J.-H. Noh et al., Three-dimensional inverse heat conduction modeling of a multi-layered hollow cylindrical tube using input estimation algorithm and thermal resistance network, Int. J. Heat Mass Transfer (2016), http://dx.doi.org/10.1016/j.ijheatmasstransfer.2016.09.101

wave is consistent with the tendency of the true value of heat flux that is actually entered. However, due to the effect of the thickness of hollow cylindrical tube, delay is noticed as the preceding result. At the maximum peak of wave, the delay time is 0.49 s, and the difference of the maximum peak is ±0.19%. Moreover, as shown in Fig. 6b displaying the predicted value of the angle direction, the difference of value in the same length direction is very little. In addition, it is predicted that the difference of delay is at a similar level.

Lastly, the solar radiation energy is assumed to locally affect external wall of the hollow cylindrical tube, and the predicted values are compared when heat flux of sinusoidal-like wave presented in Eq. (52) is provided to the inner wall of the hollow cylindrical tube. By doing so, it is verified that the internal heat flux can be predicted accurately even though the boundary condition of external wall of tube differs locally. Accordingly, convective condition is given to every part of the outer surface area while heat flux of the solar radiation energy of 100,000 W/m^2 is applied to a limited part of the outer surface area between 0 and 90 degrees. As shown in Fig. 7, it is confirmed that there is no effect on the prediction of internal heat flux as long as settings are correctly done during the inverse heat transfer analysis even though the external bound-

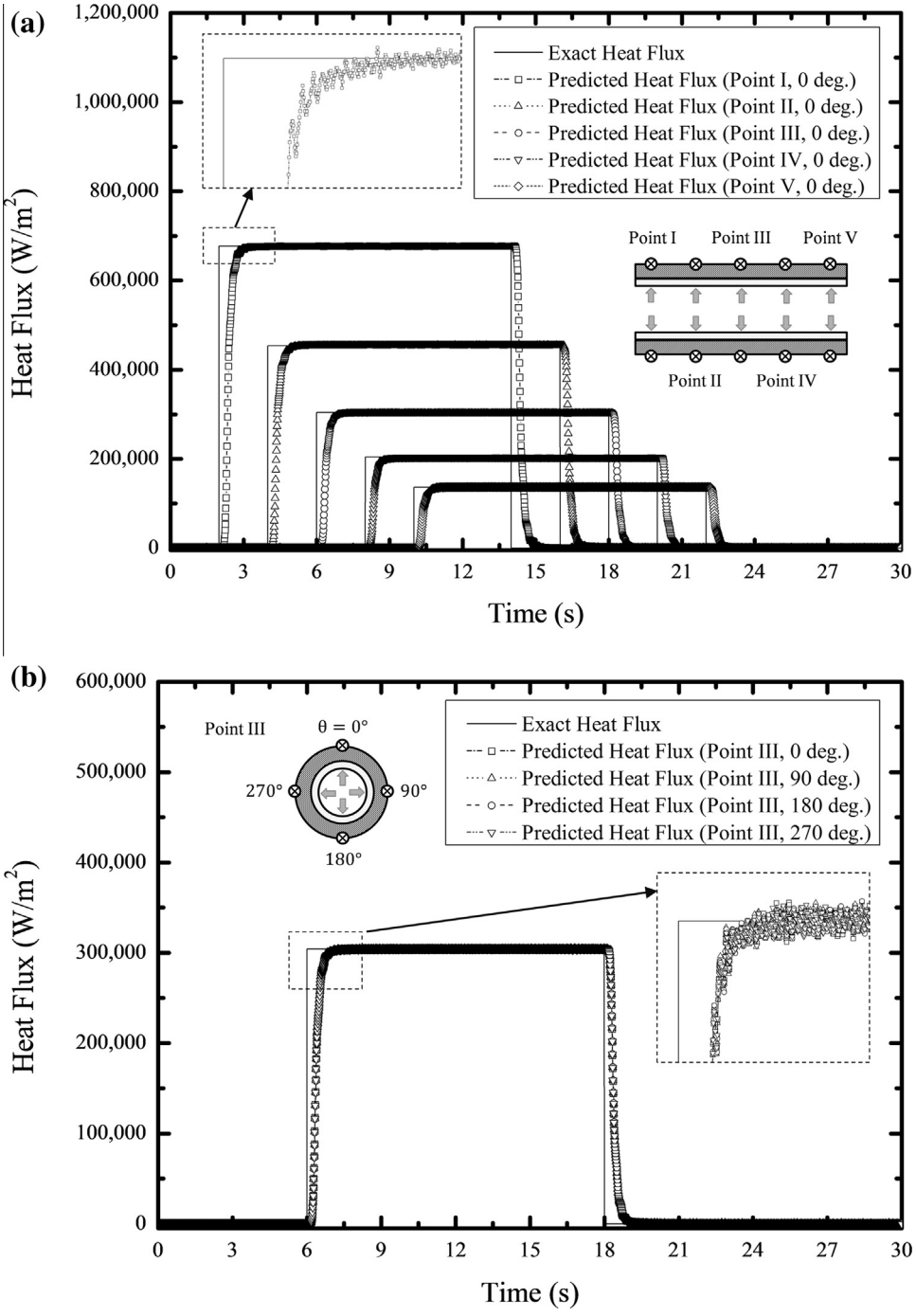

Fig. 5. Comparison between the exact heat flux profile of square wave varying according to time and the length direction of hollow cylindrical tube and the heat flux predicted by the numerical model; (a) length direction, (b) angle direction.

Please cite this article in press as: J.-H. Noh et al., Three-dimensional inverse heat conduction modeling of a multi-layered hollow cylindrical tube using input estimation algorithm and thermal resistance network, Int. J. Heat Mass Transfer (2016), http://dx.doi.org/10.1016/j.ijheatmasstransfer.2016.09.101

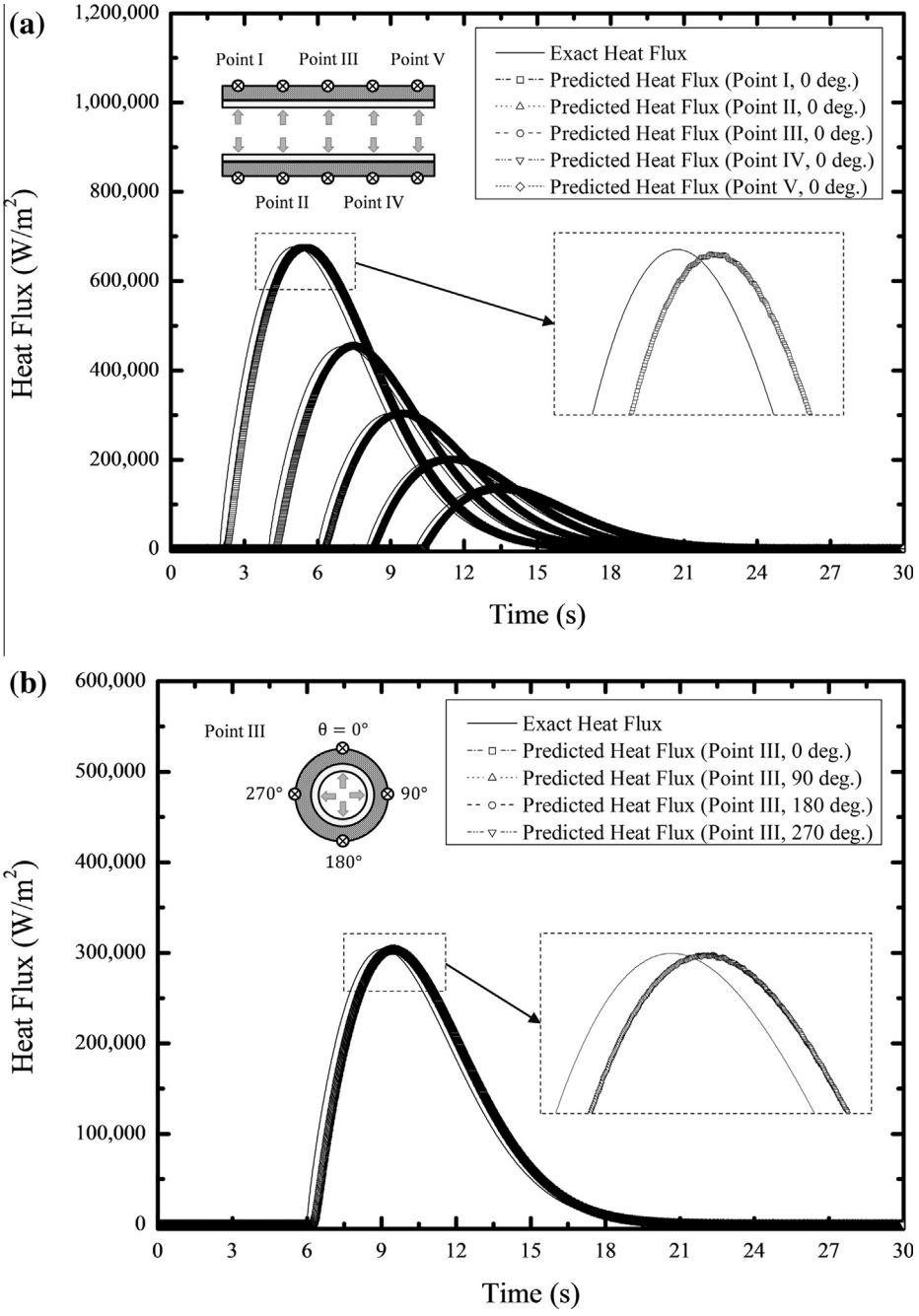

Fig. 6. Comparison between the exact heat flux profile of sinusoidal-like wave that changes according to time and the length direction of hollow cylindrical tube and the heat flux predicted by the numerical model; (a) length direction, (b) angle direction.

ary condition varies for each location, *e.g.*, locally different incidence of solar radiation. At the maximum peak of wave, delay time is 0.50 s and the difference of the maximum peak is ±0.15%.

4. Conclusions

This study focuses on the development of the three-dimensional inverse heat transfer analysis model of the hollow cylindrical tube by using the thermal resistance method and recursive input estimation algorithm. In order to verify the validity of the model developed in this study, the tube's internal temperature is measured with use of the commercial program, ANSYS FLUENT *Release 16.1*, and the tube's internal heat flux through the inverse heat transfer analysis. For the measurement of temperature, heat flux is drawn by entering temperature values from a total of twenty different locations, *i.e.*, five in the direction of length by four in the direction of angle. When the difference for stabilization of square wave, which changes only on time, is set to ±1.00% in order to verify the prediction accuracy of heat flux, the delay time is 1.01 s. On the other hand, the delay time for the stabilization of square wave that changes on both time and location is 1.02 s. The delay occurs because more time is consumed for the heat transfer as the thickness of the model shape being analyzed gets bigger or delay of prediction occurs in case of the inverse heat transfer that is predicted from temperature that is measured externally. Moreover, in order to portray the hollow cylindrical tube's heat flux that is close to the actual heat flux, a heat flux profile from the reference is adopted for evaluation, and prediction of heat flux that has dif-

Please cite this article in press as: J.-H. Noh et al., Three-dimensional inverse heat conduction modeling of a multi-layered hollow cylindrical tube using input estimation algorithm and thermal resistance network, Int. J. Heat Mass Transfer (2016), http://dx.doi.org/10.1016/j.ijheatmasstransfer.2016.09.101

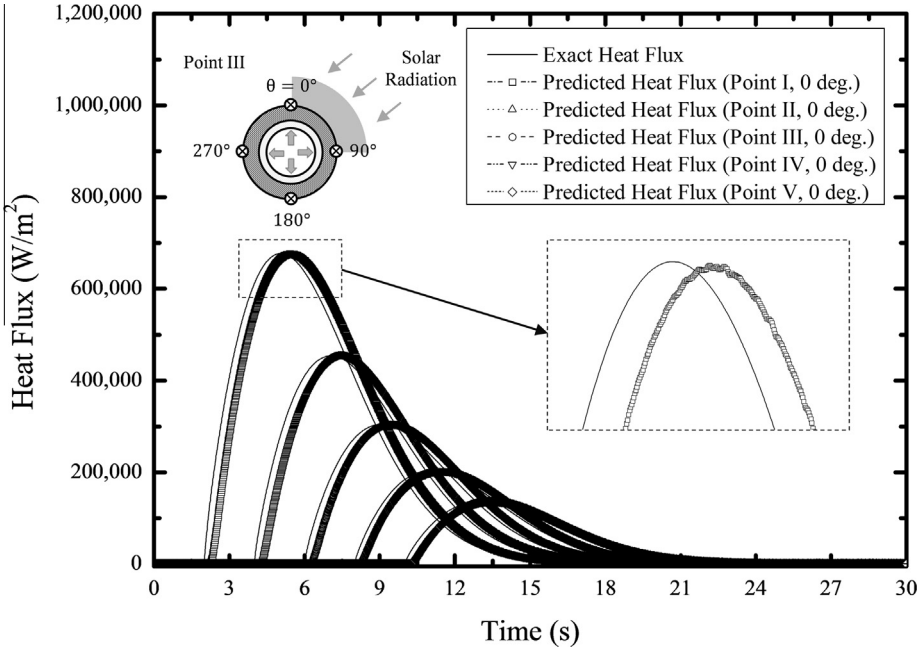

Fig. 7. Comparison between the exact heat flux profile of sinusoidal-like wave that is affected by the solar radiation energy and the heat flux predicted by the numerical model.

ference on time, location, and phase. Based on comparison of the results, it is confirmed that the delay time at the maximum peak of wave is 0.49 s, and the difference of the maximum peak is ±0.19%. It is also confirmed that, in case of sinusoidal-like wave, which has more gradual heat flux than square wave, more accurate prediction is possible, and delay time for the stabilization due to the thickness is reduced. Finally, the solar radiation energy from 0 to 90 degrees is given as a condition to verify the analysis results of the inverse heat transfer that has a non-uniform condition as an external boundary condition. It is confirmed that the delay time at the maximum peak of wave is 0.50 s, and the difference of the maximum peak is ±0.15%.

Acknowledgment

This study was supported by the Agency for Defense Development of the Republic of Korea under UE135039ID.

References

[1] G. Stolz, Numerical solution to an inverse problem of heat conduction for simple shapes, Trans. ASME J. Heat transfer 82C (1960) 20–26.
[2] E.M. Sparrow, A. Haji-Sheikh, T.S. Lundgren, The inverse problem in transient heat conduction, Trans. ASME J. Appl. Mech. 86E (1964) 369–375.
[3] J.V. Beck, Surface heat flux determination using an integral method, Nucl. Eng. Des. 7 (1968) 170–178.
[4] M. Imber, J. Khan, Prediction of transition temperature distribution with embedded thermocouples, AIAA J. 10 (1972) 784–789.
[5] K.C. Woo, L.C. Chow, Inverse heat conduction by direct inverse laplace transform, Num. Heat Transfer 4 (1981) 499–504.
[6] J.V. Beck, B. Blackwell, C.R. St. Clair, Inverse Heat Conduction, Wiley, New York, 1985.
[7] J.V. Beck, Determination of undisturbed temperatures from thermocouple measurements using correction kernels, Nucl. Eng. Des. 7 (1968) 9–12.
[8] J.V. Beck, Nonlinear estimation applied to the nonlinear inverse heat conduction problem, Int. J. Heat Mass Transfer 13 (1970) 703–716.
[9] B.F. Blackwell, Efficient technique for the numerical solution of one-dimensional inverse problem of heat conduction, Num. Heat Transfer 4 (1981) 229–238.
[10] M.O. Alifanov, V.V. Mikhailov, Solution of the nonlinear inverse thermal conductivity problem by the iteration method, J. Eng. Phys. 35 (1978) 1501–1506.
[11] Y. Jarny, M.N. Ozisik, J.P. Bardon, A general optimization method using adjoint equation for solving multidimensional inverse heat conduction, Int. J. Heat Mass Transfer 34 (1991) 2911–2919.
[12] C.H. Huang, M.N. Ozisik, Inverse problem of determining the unknown strength of an internal plane heat source, J. Franklin Inst. 329 (4) (1992) 751–764.
[13] A.J. Silva Neto, M.V. Ozisik, Simultaneous estimation of location and timewise-varying strength of a plane heat source, Numer. Heat Transfer, Part A 24 (1993) 467–477.
[14] J.C. Bokar, M.V. Ozisik, An inverse analysis for estimating the time-varying inlet temperature in laminar flow inside a parallel plate duct, Int. J. Heat Mass Transfer 38 (1) (1995) 39–45.
[15] Y.T. Chan, A.G.C. Hu, J.B. Plant, A Kalman filter based tracking scheme with input estimation, IEEE Trans. Aerospace Electron. Syst. 15 (1979) 237–244.
[16] M. Hou, S. Xian, Comments on tracking a maneuvering target using input estimation, IEEE Trans. Aerospace Electron. Syst. 25 (2) (1989) 280.
[17] P.L. Bogler, Tracking a maneuvering target using input estimation, IEEE Trans. Aerospace Electron. Syst. 15 (1979) 237–244.
[18] M. Farooo, S. Bruder, Comments on tracking a maneuvering target using input estimation, IEEE Trans. Aerospace Electron. Syst. 25 (2) (1989) 300–302.
[19] C.C. Ji, P.C. Tuan, H.Y. Jang, A recursive least-squares algorithm for on-line 1-D inverse heat conduction estimation, Int. J. Heat Mass Transfer 40 (9) (1997) 2081–2096.
[20] B.L. Wang, Y.W. Mai, Transient one-dimensional heat conduction problem solved by finite element, Int. J. Mech. Sci. 47 (2005) 303–317.
[21] N. Daouas, M.S. Radhouani, A new approach of the Kalman filter using future temperature measurements for nonlinear inverse heat conduction problem, Num. Heat Transfer 45 (2004) 565–585.
[22] T.C. Chen, C.C. Liu, H.Y. Jang, P.C. Tuan, Inverse estimation of heat flux and temperature in multi-layer gun barrel, Int. J. Heat Mass Transfer 50 (2007) 2060–2068.
[23] P.H. Mellor, D. Roberts, D.R. Turner, Lumped parameter thermal model for electrical machines of TEFC design, Electric Power Appl. 138 (5) (1991) 205–218.
[24] Smail Mezani, N. Takorabet, B. Laporte, A combined electromagnetic and thermal analysis of induction motors, IEEE Trans. Magn. 41 (5) (2005) 1572–1575.
[25] Y.A. Cengel, Heat transfer, McGraw-Hill, 2003.
[26] R.W. Lewis, P. Nithiarasu, K.N. Seetharamu, Fundamentals of the finite element method for heat and fluid flow, Wiley, 2004.
[27] T.C. Chen, C.C. Liu, Inverse estimation of time-varied heat flux and temperature on 2-D gun barrel using input estimation method with finite-element scheme, Defence Sci. J. 58 (2008) 57–76.
[28] J.H. Noh, W.G. Kim, K.U. Cha, S.J. Yook, Inverse heat transfer analysis of multi-layered tube using thermal resistance network and Kalman filter, Int. J. Heat Mass Transfer 89 (2015) 1016–1023.
[29] J.H. Noh, K.U. Cha, S.T. Ahn, S.J. Yook, Prediction of time-varying heat flux along a hollow cylindrical tube wall using recursive input estimation algorithm and thermal resistance network method, Int. J. Heat Mass Transfer 97 (2016) 232–241.

Please cite this article in press as: J.-H. Noh et al., Three-dimensional inverse heat conduction modeling of a multi-layered hollow cylindrical tube using input estimation algorithm and thermal resistance network, Int. J. Heat Mass Transfer (2016), http://dx.doi.org/10.1016/j.ijheatmasstransfer.2016.09.101